15. A. A. Shraiber, V. M. Milyutin, and V. P. Yatsenko, Hydrodynamics of Two-Component Fluids with Polydispersed Solid Material [in Russian], Kiev (1980).
16. S. M. Targ, Short Course of Theoretical Mechanics [in Russian], Moscow (1966).
17. O. Molerus, Chem. Ing. Tech., A726, No. 12, 945-955 (1977).
18. G. Welchof, VDI-Forschungsheft, 28B (492), 18-26 (1962).
19. Y. Morikawa and T. Tanaka, J. Soc. Powder Tech. Jpn., 21, No. 2, 87-94 (1984).

ANALYSIS OF MELTING IN A VERTICAL ANNULAR GAP IN CONDITIONS OF HEAT TRANSFER WITH AN INDUCED HEAT-CARRIER FLUX

V. M. Gribkov, V. M. Eroshenko, and K. V. Karmastin

UDC 536.24:536.421.1

Experimental results on the melting of materials in a vertical annular gap in conditions of heat transfer with an induced heat-carrier flux are obtained and generalized.

There has been extensive experimental and theoretical investigation of the heat transfer on melting (solidification) [1-8], paying particular attention to the influence of natural convection on the heat-transfer intensity, the determination of the phase-interface position, and the derivation of generalizing relations for the volume fraction of melt with boundary conditions of types I and II. In practice, melting (solidification) with heat transfer to an induced heat-carrier flux is of great interest. The solution of such problems is particularly urgent in creating effective and economical heat storage units operating together with various types of power equipment. At present, there is limited information available here; it basically pertains to the theoretical investigation of heat transfer in the exterior solidification of plane or cylindrical channels cooled by a heat-carrier flux [9-11]. Note that the solutions obtained take no account of the role of natural convection in the melt, whereas convection has a significant influence on the heat-transfer characteristics in melting (solidification). In addition, there are no formulas as yet for the calculation of the integral heat-transfer characteristics on melting (solidification) in conditions of induced heat-carrier flow.

The aim of the present work is to elucidate the basic laws of heat transfer on melting in a vertical annular gap in conditions of induced heat-carrier flow, and to obtain a generalizing dependence for the calculation of the stored energy.

Experimental investigation of the heat transfer on melting is undertaken on five models. Each model is a system of two vertical coaxial cylindrical tubes: a working channel and the external shell of the model. There is induced motion of the heat carrier along the working channel, and the annular gap is filled with melting material. One model is briefly described here. The working channel of the model is made from a stainless steel tube of internal diameter 2.8 mm and wall thickness 0.1 mm, with a section of hydrodynamic stabilization. At the working-chamber inlet and outlet, there are mixing chambers for measuring the heat-carrier temperature. The external shell of the model is also made from a stainless steel tube (internal diameter 25 mm; wall thickness 0.4 mm). Chromel-Copel thermocouples are welded to the outer surface of the working channel and the external shell of the model, so as to record the wall temperature distribution over the height of the model in the course of the experiments.

One basic feature of the model is the heat-insulating system, which is required to ensure adiabatic conditions at the external shell. It consists of a vacuum chamber, ohmic heaters, and a heat-insulating coating. Ohmic heaters are placed on the outer surface of

G. M. Krzhizhanovskii State Scientific-Research Power Institute, Moscow. Translated from Inzhenerno-Fizicheskii Zhurnal, Vol. 58, No. 2, pp. 214-220, February, 1990. Original article submitted February 7, 1989.

0022-0841/90/5802-0157$12.50

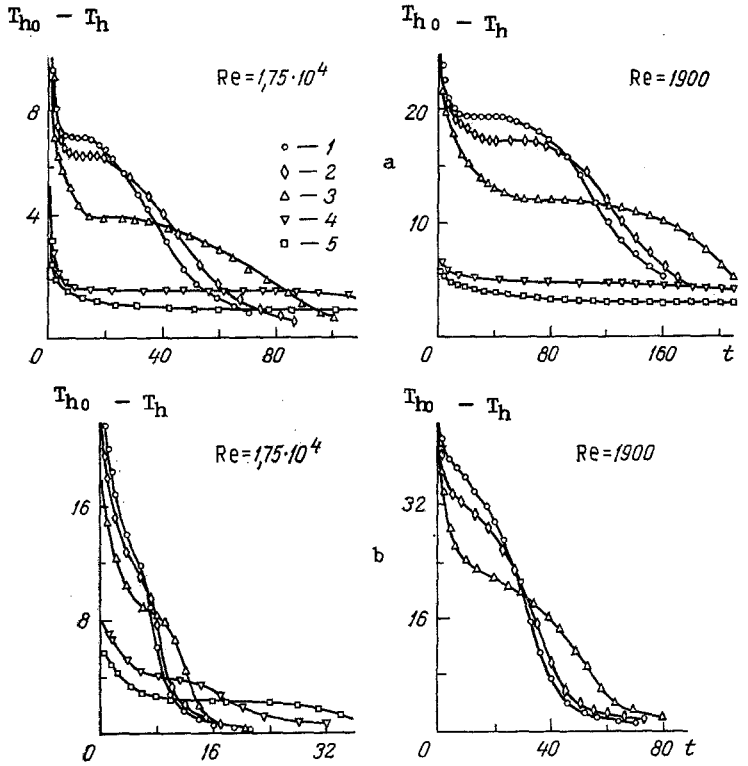

Fig. 1. Variation in temperature difference of heat carrier over time in the melting of n-eicosane on the model with ℓ/d_1 = 30 and r_2/r_1 = 8.33 (a) and with ℓ/d_1 = 90, r_2/r_1 = 3.33 (b): 1) $T_{h0} - T_0$ = 58°C, $T_m - T_0$ = 5.1°C; 2) 58.0 and 10.8; 3) 58.0 and 26.6; 4) 13.7 and 1.2; 5) 13.7 and 6.3. $T_{h0} - T_h$, °C; t, min.

the vacuum chamber and automatically maintain the surface temperature of this chamber in accordance with the temperature distribution over the height of the external shell.

The initial height of the solid sample of fusible material in all the experiments with the same model is constant. The procedure for obtaining a solid sample of fusible material and bringing it to the initial state and the experimental method were described in detail in [12].

The heat transfer is studied in conditions of constant heat-carrier flow rate and temperature at the model input and with adiabatic conditions at the external shell of the model. Gaseous nitrogen is used as the heat carrier; the fusible materials employed are n-eicosane, n-octadecane, and the crystal hydrate of zinc nitrate $Zn(NO_3)_2 \cdot 6H_2O$. The thermophysical properties of the material are determined according to [13-15]. The working parameters vary in the following ranges: Kt = 0.08-0.5; Ko = 1.8-8.0; Re = 1900-5.45·10⁴; ℓ/d_1 = 30-180; r_2/r_1 = 3.3-15.6; a_L/a_S = 1.18-1.9.

The experimental results allow the characteristic heat-transfer mechanisms to be established in the case of melting in a vertical annular gap. Consider the melting of n-eicosane in the model with ℓ/d_1 = 30 and r_2/r_1 = 8.33. The variation in heat-carrier temperature difference over time is shown in Fig. 1a for various flow conditions, total temperature differences, and degrees of supercooling of the fusible material. In the initial stage of the melting process, the dominant heat-transfer mechanism is heat conduction. In this period, sharp change in heat-carrier temperature at the model output is seen, as well as decrease in the mean heat-transfer coefficient from the wall of the working channel to the liquid melt. The thickness of the melt layer is small here, and remains practically constant over the height of the annular gap. This is confirmed by the monotonic increase in wall temperature of the working channel, varying linearly over the length.

Subsequently, as the melting front moves over the radius of the model, natural convection begins to influence the heat transfer in the melting material. At this stage, the presence of conditions with sections of constant heat-carrier temperature at the output is char-

acteristic. Sharply expressed nonlinearity is observed here in the distribution of the wall temperature over the length of the working channel, and the mean heat-transfer coefficient from the wall of the working channel to the liquid melt increases. Analysis of the combination of these phenomena shows that, in the given time interval, freely convective motion arises under the action of thermogravitation in the melt, leading to significant intensification of melting.

In the next stage of the melting process, the action of natural convection intensifies, and it becomes the predominant mechanism of heat transfer. As a result, the nonlinearity in the wall-temperature distribution of the working channel becomes more strongly expressed, and a maximum appears in the distribution of the mean heat-transfer coefficient. This period corresponds to the section of practically linear variation in the heat-carrier temperature difference. Intensification of melting on account of convection occurs up to a certain moment of time. With complete melting and heating of the material, the temperature in the annular gap is equalized, and the influence of natural convection is reduced.

Analysis of the experimental data shows that this behavior of the heat-carrier temperature at the model output is characteristic of all the curves in Fig. 1a. The quantitative differences existing in the rates of temperature variation in the initial and final stages of the process and the difference in the length of the constant-temperature section are explained by the different temperature differences and the different Re. Thus, with specified Re (for example, $Re = 1.75 \cdot 10^4$), increase in temperature difference of the heat carrier is associated with increase in the temperature difference over the height of the model and decrease in duration of the melting process (curves 1-3 in comparison with curves 4 and 5). Processes characterized by the same temperature differences of the heat carrier have different degrees of supercooling (curves 1, 2, and 3). It is evident that increase in the initial supercooling of the melting material is associated with delay in reaching the section with constant heat-carrier temperature, increase in the length of this section, and a longer process as a whole. This is because some of the energy supplied to the material increases the temperature of the solid phase. In this case, a small temperature difference between T_w and T_m is realized, significantly retarding the melting process.

The influence of the heat-carrier flow conditions on the heat transfer in melting is now investigated. As shown by experimental results, variation in Re in the range $1900 \leq Re \leq 1.75 \cdot 10^4$ leads to no qualitative change in the behavior of the heat-carrier temperature at the model output, but the quantitative differences are significant, as a result of the different heat-transfer coefficients for the different processes. Increase in heat-transfer coefficient leads to reduction in thermal resistance from the heat-carrier flux, which results in a larger wall temperature of the working channel for conditions with large Re in a specified time interval and hence to more rapid development of melting.

Analysis of the influence of the relative height of the model on the heat transfer is now analyzed. To this end, the experimental data obtained on models with $\ell/d_1 = 30$ and $\ell/d_1 = 90$ when $r_2/r_1 = 8.33$, and with $\ell/d_1 = 90$ and $\ell/d_1 = 180$ when $r_2/r_1 = 3.33$, are compared. The comparison shows that increase in ℓ/d_1 results in no qualitative change in the behavior ring at large ℓ/d_1 are distinguished by a larger temperature difference, greater length of

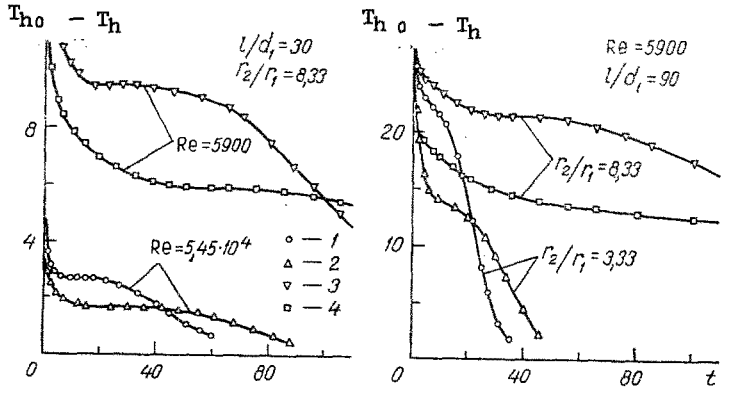

Fig. 2. Variation in temperature difference of heat carrier over time in the melting of $Zn(NO_3)_2 \cdot 6H_2O$: 1, 3) $T_{h_0} - T_0 = 32.4°C$; $T_m - T_0 = 2.85°C$; 2, 4) 32.4 and 14.9.

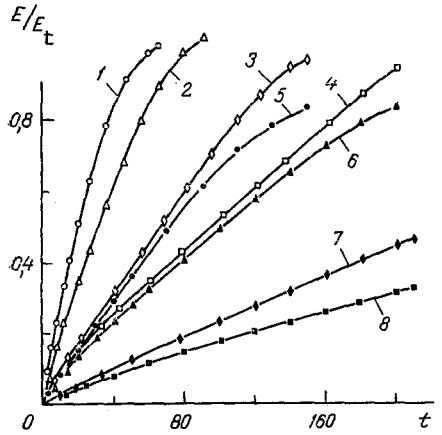

Fig. 3. Variation in stored energy over time for the model with $\ell/d_1 = 30$ and $r_2/r_1 = 8.33$: 1-4) $Re = 1.75 \cdot 10^4$; 5-8) $Re = 1900$; 1, 5) $T_{h_0} - T_0 = 58.0°C$, $T_m - T_0 = 5.1°C$; 2, 6) 58.0 and 26.7; 3, 7) 13.7 and 1.2; 4, 8) 13.7 and 6.3.

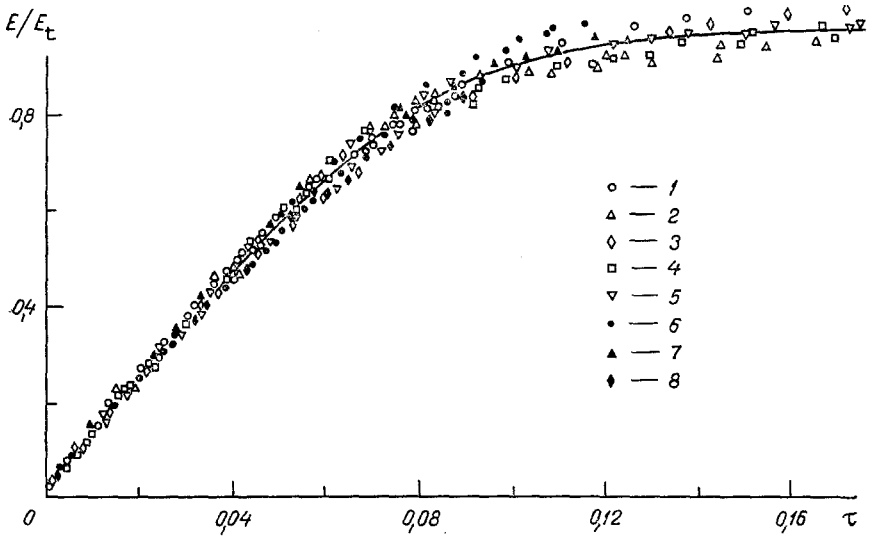

Fig. 4. Generalization of experimental data on the melting of various materials in a vertical annular gap: Kt = 0.08-0.50, Ko = 1.8-8.0, $Re = 1900\text{-}5.45 \cdot 10^4$; 1-4) n-eicosane; 5) n-octadecane; 6-8) zinc nitrate crystal hydrate; 1, 6) $\ell/d_1 = 30$; $r_2/r_1 = 8.33$; 2, 7) 90 and 3.33; 3, 8) 90 and 8.33; 4) 90 and 15.62; 5) 180 and 3.33.

the section with constant heat-carrier temperature, and greater duration of the melting process. The relation between ℓ/d_1 and these quantities is not linear.

In investigating the influence of the relative width of the annular gap on the heat transfer in melting, a characteristic feature of the processes is established: decrease in r_2/r_1 to $r_2/r_1 = 3.33$ leads to transition from conditions with sections of constant heat-carrier temperature to conditions with linear variation in flow temperature. This is clearly evident in Fig. 1b. In the initial stage of melting, the processes are similar to melting in the model with $r_2/r_1 = 8.33$. Then, in the model with $r_2/r_1 = 3.33$, no transition to conditions with constant heat-carrier temperature is seen, but there is linear variation in flow temperature for a certain period of time. This is because the decrease in the annular gap leads to decrease in the influence of natural convection on the heat transfer in melting. The character of the change in flow temperature is not influenced, however, by the conditions of heat-carrier flow and the relative height of the model. Decrease or increase in Re and ℓ/d_1 lead only to quantitative differences in the length of the melting process

and in the temperature difference. With increase in r_2/r_1 from 8.33 to 15.6, there are no qualitative changes in the melting process. All that need be noted here is that the sections with constant heat-carrier temperature become clearly expressed in this case.

All the foregoing also applies for the heat transfer in the melting of material with higher thermal conductivity and viscosity in comparison with hydrocarbons. This is confirmed by experiments on the same models using hydrated crystals of zinc nitrate $Zn(NO_3)_s \cdot 6H_2O$ as the fusible material (Fig. 2). The results of the investigation show that, for processes with $r_2/r_1 = 8.33$, regardless of Re and ℓ/d_1, the presence of sections with constant flow temperature is characteristic, as before; for processes with $r_2/r_1 = 3.33$, transition to linear variation in heat-carrier temperature is characteristic. Decrease in the thermal resistance from the fusible material leads only to overall reduction in temperature difference of the heat carrier and to reduction in the duration of melting for all models and conditions, in comparison with the use of materials with lower thermal diffusivity and viscosity.

Consider the energy transfer from the heat carrier to the melting material. On the basis of the conditions of the problem, the energy supplied by the heat carrier is the energy stored in the model for the given time energy. The change in stored energy on melting is now analyzed for the model with $\ell/d_1 = 30$ and $r_2/r_1 = 8.33$ (Fig. 3). The curves in Fig. 3 characterize the intensity of various melting processes: with increase in the relative stored energy (E/E_t) in the given time period, there is increase in the energy transfer by the heat carrier to the melting material and increase in rate of the melting process. As is evident, processes characterized by large total temperature differences occur more intensively (curves 1 and 2 in comparison with curves 3 and 4). Increase in Re leads to an analogous result (curves 1-4 in comparison with curves 5-8, respectively). Analysis of the experimental data also shows that increase in the initial supercooling of the material (curves 2, 4 and 6, 8 in comparison with curves 1, 3 and 5, 7, respectively) is associated with decrease in stored energy in the given time interval and hence decrease in intensity of the process.

Analysis of experimental data on the influence of various determining factors on the heat transfer for melting in a vertical annular gap permits the determination of the form of the functional dependence, which is used to generalize the results obtained (Fig. 4). Note that the variation in relative width of an annular gap in the range $3.3 \leq r_2/r_1 \leq 15.6$ has no influence on the rate of melting. The dependence of the stored energy on the dimensionless time for these cases is the same. Thus, it may be asserted that the influence of r_2/r_1 on the energy accumulation is slight.

Analysis of the experimental results by the least-squares method gives a generalizing dependence of the form

$$E/E_t = \sum_{n=0}^{4} A_n [1 - \exp(-40\tau^{1.3})]^n, \quad (1)$$

where $A_0 = 4.6 \cdot 10^{-3}$; $A_1 = 1.65$; $A_2 = -3.11$; $A_3 = 5.0$; $A_4 = -2.56$; $\tau = \tau^* Kt^{-0.21} Re^{-0.37} \cdot (\ell/d_1)^{-0.24} (a_L/a_S)^{-0.55}$.

A generalization of the experimental data described by Eq. (1) with an accuracy of ±8% is shown in Fig. 4. An expression generalizing the experimental data with the same accuracy may be recommended, for convenience of calculation

$$E/E_t = 1 - \exp(-B\tau^k),$$

where $B = 22.4$, $k = 1.0$ when $\tau \leq 0.047$; $B = 76.0$, $k = 1.50$ when $\tau \geq 0.047$.

The results obtained are valid in a narrow range of variation of the basic parameters, and may be used to calculate the heat transfer on melting in a vertical annular gap, in conditions of induced heat-carrier flow.

NOTATION

ℓ, length of working channel of model; r_1, radius of working channel of model; r_2, radius of external shell of the model; T, temperature; c, specific heat; h, heat of melting; λ, thermal conductivity; a, thermal diffusivity; t, time; m, m_s, mass of melting material and mass of structure; G, mass flow rate; $Kt = (T_m - T_\ell)/(T_{h0} - T_0)$, degree of supercooling of melting material; $Ko = h/[c_L(T_{h0} - T_0)]$, Koso-

vich number; $E = Gc_h \sum_{i=1}^{n} [T_{h^0} + \frac{1}{2}(T_{h^{i-1}} + T_{h^i})]\Delta t_i$, stored energy; $E_t = m[c_S(T_m - T_0) + h + c_L(T_{ho} - T_m)] + m_s c_s (T_{h^0} - T_0)$, total amount of energy; $\tau^* = \mathrm{Nu}(T_{h^0} - T_0)\pi l/\lambda_h \times t/Et$, dimensionless time. Subscripts: 0, initial state; m, melting; L, liquid phase; S, solid phase; h, heat carrier; w, wall; s, structure.

LITERATURE CITED

1. R. G. Kemink and E. M. Sparrow, Int. J. Heat Mass Trans., 24, No. 10, 1699-1710 (1981).
2. Sparrow and Broadbent, Teplopered., 104, No. 2, 85-92 (1982).
3. M. Okada, Int. J. Heat Mass Trans., 27, No. 11, 2057-2066 (1984).
4. Kho and Viskanta, Teplopered., 106, No. 1, 9-18 (1984).
5. Kal'khori and Ramad'yani, Teplopered., 107, No. 1, 42-50 (1985).
6. Benar, Goben, and Martines, Teplopered., 107, No. 4, 49-58 (1985).
7. Go and Viskanta, Teplopered., 108, No. 1, 159-166 (1986).
8. Sparrow, Gertshed, and Mairam, Teplopered., 108, No. 3, 142-147 (1986).
9. E. M. Sparrow and C. F. Hsu, Int. J. Heat Mass Trans., 24, No. 8, 1345-1357 (1981).
10. Hsu and Sparrow, Teplopered., 103, No. 3, 231-233 (1981).
11. N. Shamsundar, Int. J. Heat Mass Trans., 25, No. 10, 1614-1616 (1982).
12. K. V. Karmastin and V. A. Kuznetsov, Energy Storage and Means of Increasing the Operating Efficiency of Power Stations and Energy Savings: Proceedings of an All-Union Scientific Conference [in Russian], Moscow, Part II, pp. 136-144 (1986).
13. W. R. Humphries and E. I. Griggs, NASA Technical Paper, No. 1074 (1977).
14. S. K. Jain, J. Chem. Eng. Data, 23, No. 2, 170-173 (1978).
15. J. Guion, J. D. Sauzade, and M. Laugt, Thermochim. Acta, 67, No. 2, 167-179 (1983).

ACCURATE SOLUTIONS OF BOUNDARY-LAYER EQUATIONS FOR MOVING PERMEABLE SURFACES

G. I. Burdé

UDC 532.526

New accurate solutions of the equations of a laminar boundary layer are obtained for steady flow induced by the motion of a continuous solid surface at constant velocity.

The flow arising in the motion of a solid surface in a quiescent liquid is of interest in connection with film and fiber production in the glass and polymer industries. The boundary layers at continuous surfaces moving at constant velocity in a viscous incompressible liquid were considered in [1-5]. In [1-4], the flow close to impermeable plane and cylindrical surfaces was studied. In the case of a plane surface, when there is a self-similar solution, the problem reduces to numerical integration of an ordinary differential equation [1, 2]. In the case of a cylindrical surface, the solution is obtained by the integral method [1, 3] and the method of expansion in power series with respect to the radial coordinate [4]. In [5], the self-similar solution was investigated numerically for a boundary layer at a permeable plane surface, through which there is suction or injection of the same liquid at a velocity decreasing in the direction of motion of the plane according to the law $v_0 = q/\sqrt{x}$.

The present work gives some accurate solutions of the equations of a laminar boundary layer of incompressible liquid, describing the flow close to permeable surfaces moving at constant velocity; these solutions exist in the presence of a definite relation between the liquid suction rate and the other parameters of the problem. The solution for the case of a cylindrical surface gives a sufficiently rare example of an accurate non-self-similar solution.

The boundary-layer equations for a flow induced by the motion of a plane surface in

Perm' State Pedagogical Institute.

Translated from Inzhenerno-Fizicheskii Zhurnal, Vol. 58, No. 2, pp. 220-223, February, 1990. Original article submitted September 19, 1988.

0022-0841/90/5802-0162$12.50